ELSEVIER

Physica D 168–169 (2002) 205–219

PHYSICA D

www.elsevier.com/locate/physd

Current reversals in deterministic ratchets: points and dimers

José L. Mateos*

Instituto de Física, Universidad Nacional Autónoma de México, Apartado Postal 20-364, 01000 Mexico, DF, Mexico

Abstract

We address the problem of the chaotic transport of point particles and rigid dimers in an asymmetric periodic ratchet potential. When the inertial term is taken into account, the dynamics can be chaotic and modify the transport properties. By a comparison between the bifurcation diagram and the current, we identify the origin of the multiple current reversals as bifurcations, usually from a chaotic to a periodic regime. We consider the dynamics of rigid dimers, as a function of size, extending in this way our previous results for point particles.

PACS: 05.45.Ac; 05.40.Fb; 05.45.Pq; 05.60.Cd

Keywords: Deterministic ratchets; Chaotic transport; Current reversals

1. Introduction

There is an increasing interest in recent years in the study of the transport properties of nonlinear systems that can extract usable work from unbiased non-equilibrium fluctuations. These so-called ratchet systems can be modeled, for instance, by considering a Brownian particle in a periodic asymmetric potential and acted upon by an external time-dependent force of zero average. This recent burst of work is motivated in part by the challenge to explain the unidirectional transport of molecular motors in the biological realm and the possibility for new methods of separation of particles. For recent reviews, see [1–4].

Although the vast majority of the literature in this field considers the presence of noise, very recently there has been motivations to understand in detail the transport properties of classical *deterministic inertial ratchets* [5–21]. These ratchets have in general a classical chaotic dynamics that determines the transport properties. The implications of this chaotic dynamics in deterministic ratchets have recently been address in the quantum domain, together with the possible connection with quantum chaos [22–24].

In particular, in a recent paper [6] we established, for the first time, a connection between the current generated in a deterministic rocking ratchet and the bifurcation diagram associated with chaotic dynamics. It turns out that when we plot the current, defined as an average velocity, against a control parameter of the system, we found multiple current reversals; on the other hand, we can obtain a bifurcation diagram plotting the velocity of the particle as a function of the same control parameter. We notice a clear connection between these two plots and by doing a close comparison we found that the current reversals occur associated with bifurcations. In many cases, these reversals occur in crisis bifurcations from a chaotic to a periodic regime.

It is worth mentioning that this prediction has been verified qualitatively in a recent experiment done by

* Tel.: +52-5-622-5130; fax: +52-5-622-5015.
E-mail address: mateos@fisica.unam.mx (J.L. Mateos).

0167-2789/02/$ – see front matter
PII: S0167-2789(02)00510-9

Carapella et al. [20], using the ratchet effect for a relativistic flux quantum trapped in an annular Josephson junction embedded in an inhomogeneous magnetic field.

In this paper, we elaborate on this idea by studying current reversals and bifurcations for point particles and extended rigid dimers. We analyze trajectories and orbits in phase space for point particles. We also present current reversals, as a function of the size of the rigid dimers, together with the corresponding bifurcation diagram.

The outline of the paper is as follows: in Section 2, we introduce the equations of motion that define the model and in Section 3 we present the numerical results. Then we study the case of extended objects in Section 4 and finally we end with some concluding remarks in Section 5.

2. The ratchet potential model

Let us consider the one-dimensional problem of a particle driven by a periodic time-dependent external force, under the influence of an asymmetric periodic potential of the ratchet type. The time average of the external force is zero. Here, we do not take into account any kind of noise and thus the dynamics is deterministic. The equation of motion is given by

$$m\ddot{x} + \gamma\dot{x} + \frac{\mathrm{d}V(x)}{\mathrm{d}x} = F_0 \cos(\omega_D t), \tag{1}$$

where m is the mass of the particle, γ the friction coefficient, $V(x)$ the external asymmetric periodic potential, F_0 the amplitude of the external force and ω_D the frequency of the external driving force. The ratchet potential is given by

$$V(x) = V_1 - V_0 \sin\frac{2\pi(x - x_0)}{L} - \frac{V_0}{4}\sin\frac{4\pi(x - x_0)}{L}, \tag{2}$$

where L is the periodicity of the potential, V_0 the amplitude and V_1 an arbitrary constant. The potential is shifted by an amount x_0 in order that the minimum of the potential is located at the origin.

Let us define the following dimensionless units: $x' = x/L$, $x'_0 = x_0/L$, $t' = \omega_0 t$, $w = \omega_D/\omega_0$, $b = \gamma/m\omega_0$ and $a = F_0/mL\omega_0^2$. Here, the frequency ω_0 is given by $\omega_0^2 = 4\pi^2 V_0\delta/mL^2$ and δ is defined by $\delta = \sin(2\pi|x'_0|) + \sin(4\pi|x'_0|)$.

The frequency ω_0 is the frequency of the linearized motion around the minima of the potential, thus we are scaling the time with the natural period of motion $\tau_0 = 2\pi/\omega_0$. The dimensionless equation of motion, after renaming the variables again without the primes, becomes

$$\ddot{x} + b\dot{x} + \frac{\mathrm{d}V(x)}{\mathrm{d}x} = a\cos(wt), \tag{3}$$

where the dimensionless potential can be written as

$$V(x) = C - \frac{1}{4\pi^2\delta}\left[\sin 2\pi(x - x_0) + \frac{1}{4}\sin 4\pi(x - x_0)\right], \tag{4}$$

and is depicted in Fig. 1. The constant C is such that $V(0) = 0$ and is given by $C = -(\sin 2\pi x_0 + 0.25\sin 4\pi x_0)/4\pi^2\delta$. In this case, $x_0 \simeq -0.19$, $\delta \simeq 1.6$ and $C \simeq 0.0173$.

In the equation of motion (3), there are three dimensionless parameters: a, b and w, defined above in terms of physical quantities. The parameter $a = F_0/mL\omega_0^2$ is the ratio of the amplitude of the external force and the force due to the potential $V(x)$. This can be seen more clearly using the expression for ω_0^2 in terms of the parameters of the potential. In this case, the ratio

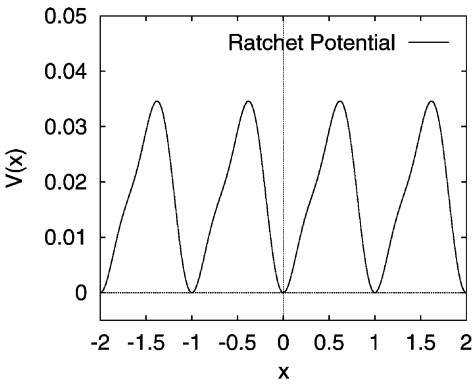

Fig. 1. The dimensionless ratchet periodic potential $V(x)$.

becomes

$$a = \frac{1}{4\pi^2\delta}\frac{F_0 L}{V_0}, \tag{5}$$

i.e., except for a constant factor, a is the ratio of F_0 and the force V_0/L, where V_0 is the amplitude and L the periodicity of the potential (see Eq. (2)). The parameter b is simply the dimensionless friction coefficient and w the ratio of the driving frequency of the external force and ω_0.

The extended phase space in which the dynamics is taking place is three-dimensional, since we are dealing with an inhomogeneous differential equation with an explicit time dependence. This equation can be written as a three-dimensional dynamical system, that we solve numerically, using the fourth-order Runge–Kutta algorithm. The equation of motion (3) is nonlinear and thus allows the possibility of periodic and chaotic orbits. If the inertial term associated with the second derivative $\ddot{x}$ was absent, then the dynamical system could not be chaotic.

The main motivation behind this work is to study in detail the origin of the current reversal in a chaotically deterministic rocked ratchet as found in [6]. In order to do so, we have to study first the current J itself, that we define as the time average of the average velocity over an ensemble of initial conditions. Therefore, the current involves two different averages: the first average is over M initial conditions, that we take equally distributed in space, centered around the origin and with an initial velocity equal to zero. For a fixed time, say t_j, we obtain an average velocity, that we denoted as v_j, and is given by

$$v_j = \frac{1}{M}\sum_{i=1}^{M} \dot{x}_i(t_j). \tag{6}$$

The second average is a time average; since we take a discrete time for the numerical solution of the equation of motion, we have a discrete finite set of N different times t_j; then the current can be defined as

$$J = \frac{1}{N}\sum_{j=1}^{N} v_j. \tag{7}$$

This quantity is a single number for a fixed set of parameters a, b, w.

Besides the orbits in the extended phase space, we can obtain the Poincaré section, using as a stroboscopic time the period of oscillation of the external force. With the aid of Poincaré sections, we can distinguish between periodic and chaotic orbits and we can obtain a bifurcation diagram as a function of the parameter a. As was shown in [6], there is a connection between the bifurcation diagram and the current.

3. Numerical results

Using the definition of the current J given in the previous section, we calculate J fixing the parameters $b = 0.1$ and $w = 0.67$ and varying the parameter a. The current shows, as stressed before [5,6], multiple current reversals and a complex variation with a, as shown in Fig. 2. We can observe strong fluctuations as well as portions where the current is approximately constant. The challenge here is to explain this high variability in the current with the aid of what we know from the nonlinear chaotic dynamics of the system.

In order to understand the first reversal of the current, let us analyze a range of values of a between 0.065 and 0.085; we chose $b = 0.1$ and $w = 0.67$. In Fig. 3a, we show the bifurcation diagram as a function of a and in Fig. 3b we depict the current in the same range of a. Let us imagine that an ensemble of particles are initially located at the minimum of the ratchet potential around the origin, and that all these particles have an initial velocity equal to zero. For $a = 0$, we have no external force and thus, all these particles remain in the minimum around the origin and therefore the current is zero. For very small values of a, we still have a zero current, since the particles have friction and tend to oscillate in this minimum. However, there is a critical value of a for which the particles start to overcome the potential barriers around the minimum and transport along the ratchet potential in a periodic or chaotic way.

At the beginning, the current is dominated by transport due to periodic orbits, but for larger values of a, some of the orbits in the ensemble become chaotic and the transport is not as efficient as before, resulting in a current that starts to oscillate erratically. In

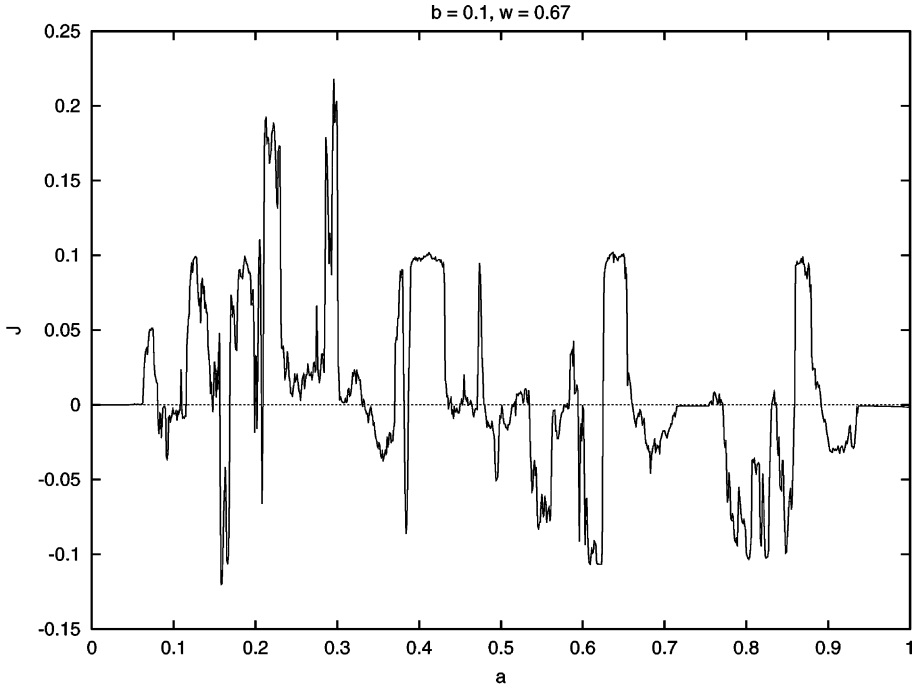

Fig. 2. For $b = 0.1$ and $w = 0.67$ we show the current J as a function of a. We can see multiple current reversals.

fact, in this region, there exist the possibility of coexistence of multiple attractors in the phase space. For example, in Fig. 3a, we have two coexistent attractors: a periodic and a chaotic one, around $a = 0.067$. In this case, depending on the initial conditions, some orbits in the ensemble can end up in the periodic attractor, and the rest in the chaotic attractor. In general, the current can depend on which basin of attraction one is located, because different attractors have different transport properties. For example, one attractor can transport particles in the positive direction, while the other in the negative direction.

For values of a even larger, all the orbits enter a chaotic region through a period-doubling bifurcation, and the current starts to decrease inside this chaotic band. Finally, exactly at the bifurcation point where a periodic window opens, the current drops to zero and becomes negative in a very abrupt way.

Let us focus first on the range of the control parameter where the first current reversal takes place. This occurs around $a \simeq 0.08$ as shown in Fig. 3. We can observe a period-doubling route to chaos and after a chaotic region, there is a crisis bifurcation (see [25]) taking place at the critical value $a_c \simeq 0.08092844$. It is precisely at this bifurcation point that the current reversal occurs. After this bifurcation, a periodic window emerges, with an orbit of period 4. In Figs. 3a and b, we are analyzing only a short range of values of a, where the first current reversal takes place. If we vary a further, we can obtain multiple current reversals, as shown in Fig. 2.

In order to understand in more detail the nature of the current reversal, let us look at the orbits just before and after the transition. The reversal occurs at the critical value $a_c \simeq 0.08092844$. If a is below this critical value a_c, say $a = 0.07$, then the orbit is periodic, with period 2. For this case we depict, in Fig. 4a, the position of the particle as a function of time. We notice a period-2 orbit, as can be distinguish in the bifurcation diagram for $a = 0.07$. This orbit transport particles to the positive direction and the corresponding velocity is a periodic function of time of period 2, as shown in Fig. 4b. The phase space for this orbit is depicted in Fig. 4c. We notice that the particle oscillates for a

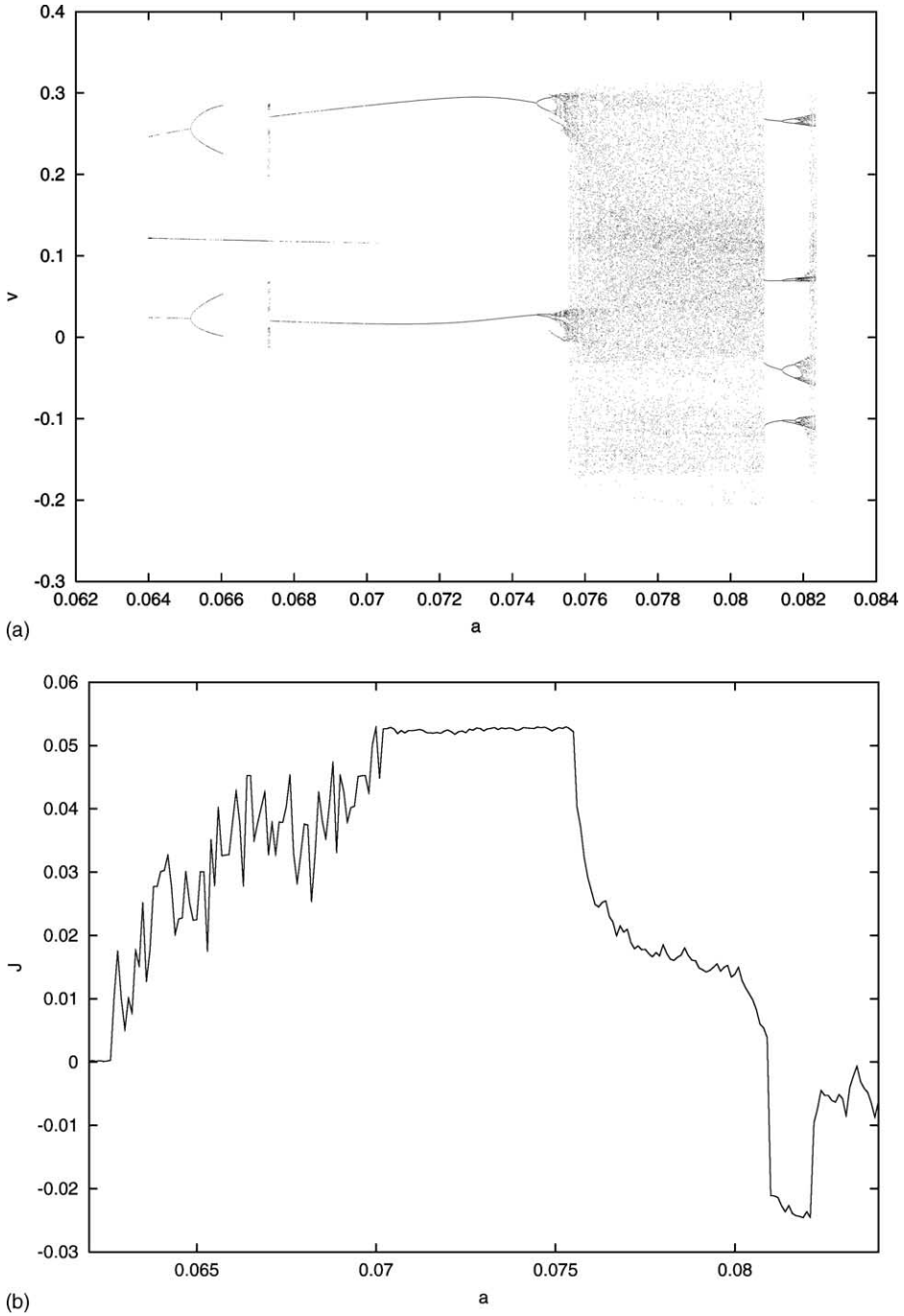

Fig. 3. For $b = 0.1$ and $w = 0.67$ we show: (a) the bifurcation diagram as a function of a and (b) the current J as a function of a. The range in the parameter a corresponds to the first current reversal.

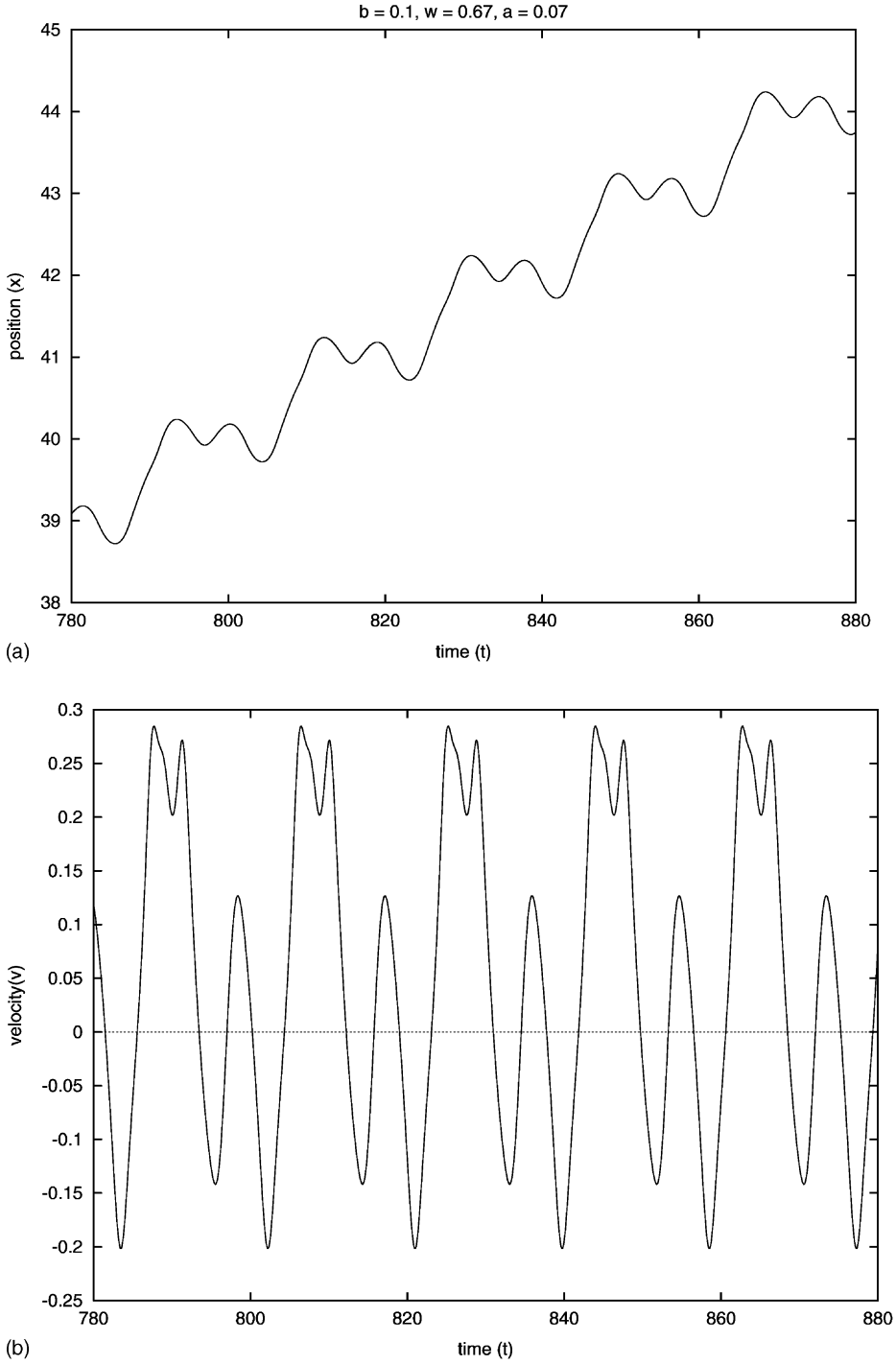

Fig. 4. For $b = 0.1$, $w = 0.67$ and $a = 0.07$ we show: (a) the trajectory of the particle as a function of time, (b) the velocity as a function of time and (c) the phase space. This case corresponds to positive current.

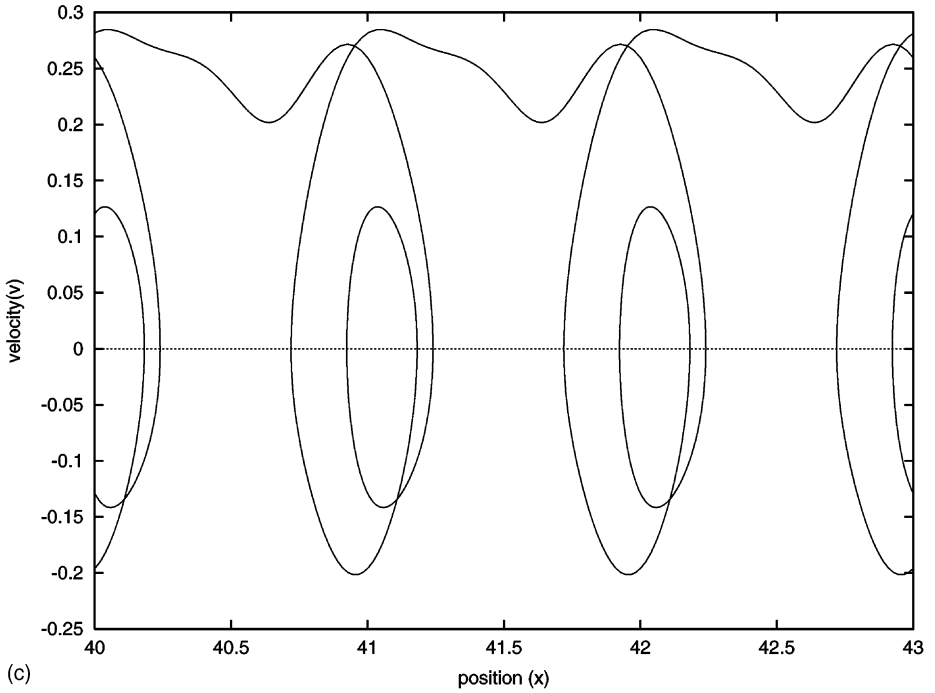

Fig. 4. (*Continued*).

while around the minima of the ratchet potential, before moving to the next one. The spatial asymmetry of the potential is apparent in this orbit in phase space.

In Fig. 5a, we show again the position as a function of time for $a = 0.081$, which is just above the critical value a_c. In this case, we observe a period-4 orbit that corresponds to the periodic window in the bifurcation diagram in Fig. 3a. This orbit is such that the particle is "climbing" in the negative direction, i.e., in the direction in which the slope of the potential is higher. We notice that there is a qualitative difference between the periodic orbit that transport particles to the positive direction and the periodic orbit that transport particles to the negative direction: in the latter case, the particle requires twice the time than in the former case, to advances one well in the ratchet potential. A closer look at the trajectory in Fig. 5a reveals the "trick" that the particle uses to navigate in the negative direction: in order to advance one step to the left, it moves first one step to the right and then two steps to the left. The net result is a negative current.

The period-4 orbit is apparent in Fig. 5b, where we show the velocity as a function of time. In Fig. 5c, we depict the corresponding phase space for this case. The transporting orbit is more elaborate because it involves motion to the positive and negative directions, as well as oscillations around the minima. In Fig. 6a, we show a typical trajectory for a just below a_c. The trajectory is chaotic and the corresponding chaotic attractor is depicted in Fig. 7. In this case, the particle starts at the origin with no velocity; it jumps from one well in the ratchet potential to another well to the right or to the left in a chaotic way. The particle gets trapped, oscillating for a while in a minimum (sticking mode), as is indicated by the integer values of x in the ordinate, and suddenly starts a running mode with average constant velocity in the negative direction. In terms of the velocity, these running modes, as the one depicted in Fig. 5a, correspond to periodic motion. This can be seen more clearly in Fig. 6b, where we plot the velocity as a function of time in the same range of values as the orbit in

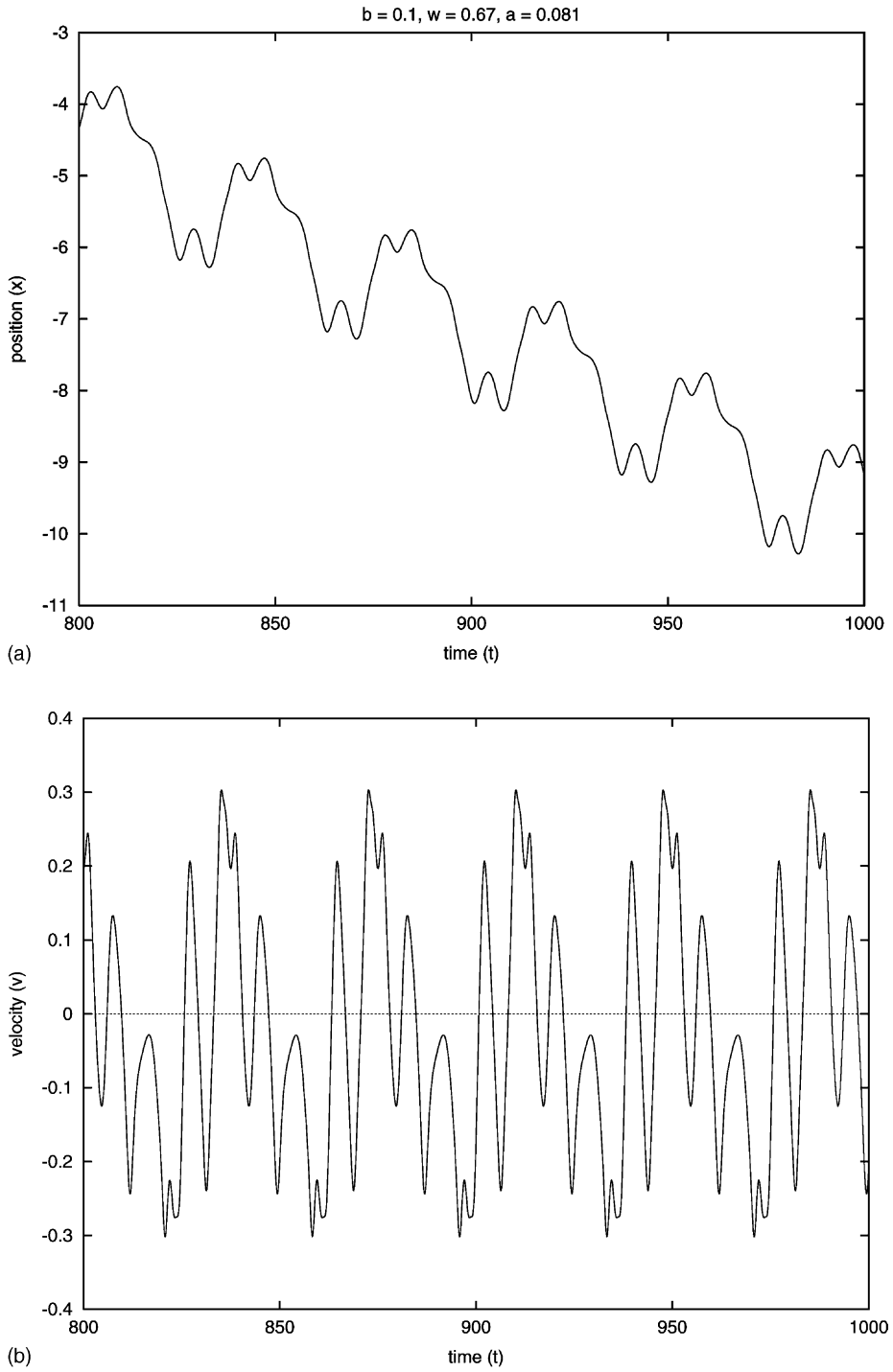

Fig. 5. For $b = 0.1$, $w = 0.67$ and $a = 0.081$ we show: (a) the trajectory of the particle as a function of time, (b) the velocity as a function of time and (c) the phase space. This case corresponds to negative current.

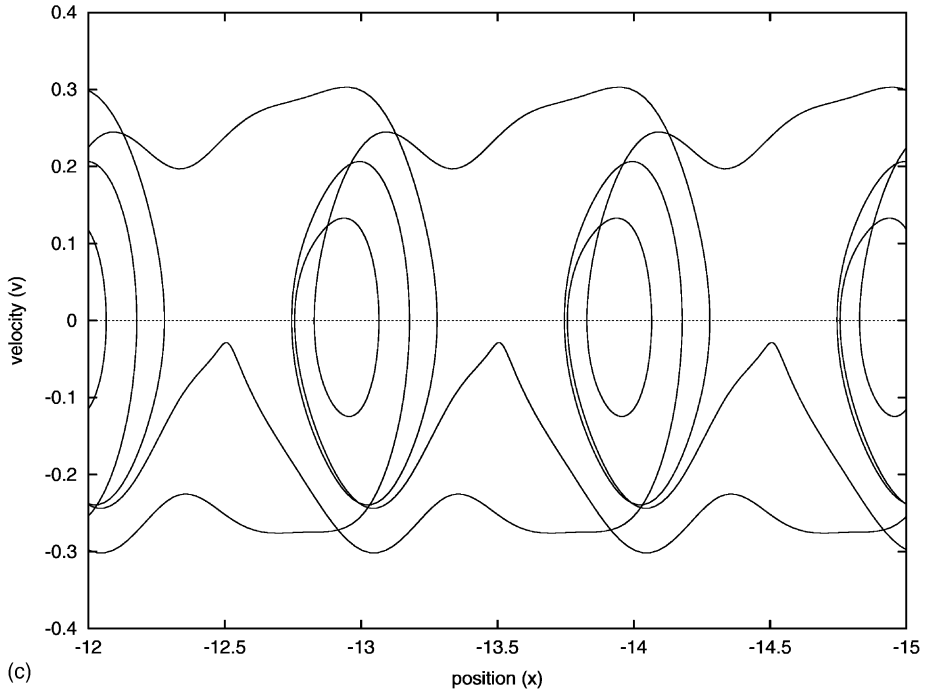

Fig. 5. (*Continued*).

Fig. 6a. In Fig. 6c, we show the corresponding phase space.

The phenomenology can be described as follows. For values of a above a_c, as in Fig. 5a, the attractor is a periodic orbit. For a slightly less than a_c there are long stretches of time (running or laminar modes) during which the orbit appears to be periodic and closely resembles the orbit for $a > a_c$, but this regular (approximately periodic) behavior is *intermittently* interrupted by finite duration "bursts" in which the orbit behaves in a chaotic manner. The net result in the velocity is a set of periodic stretches of time interrupted by burst of chaotic motion, signaling precisely the phenomenon of *intermittency* [25]. As a approach a_c from below, the duration of the running modes in the negative direction increases, until the duration diverges at $a = a_c$, where the trajectory becomes truly periodic.

To complete this picture, in Fig. 7, we show two attractors: (1) the chaotic attractor for $a = 0.08092$, just below a_c, corresponding to the trajectory in Fig. 6a, and (2) the period-4 attractor for $a = 0.08093$, corresponding to the trajectory in Fig. 5a. This periodic attractor consists of four points in phase space, which are located at the center of the open circles. We obtain these attractors confining the dynamics in x between -0.5 and 0.5, i.e., we used the periodicity of the potential $V(x+1) = V(x)$, to map the points in the x-axis modulo 1. Thus, even though the trajectory transport particles to infinity, when we confine the dynamics, the chaotic structure of the attractor is apparent. As a approaches a_c from below, the dynamics in the attractor becomes intermittent, spending most of the time in the vicinity of the period-4 attractor, and suddenly "jumping" in a chaotic way for some time, and then returning close to the period-4 attractor again, and so on. In terms of the velocity, the result is an intermittent time series as the one depicted in Fig. 6b.

In order to characterize the deterministic diffusion in this regime, we calculate the mean square displacement $\langle (x - \langle x \rangle)^2 \rangle$ as a function of time. We obtain numerically that $\langle (x - \langle x \rangle)^2 \rangle \sim t^{\alpha}$, where the

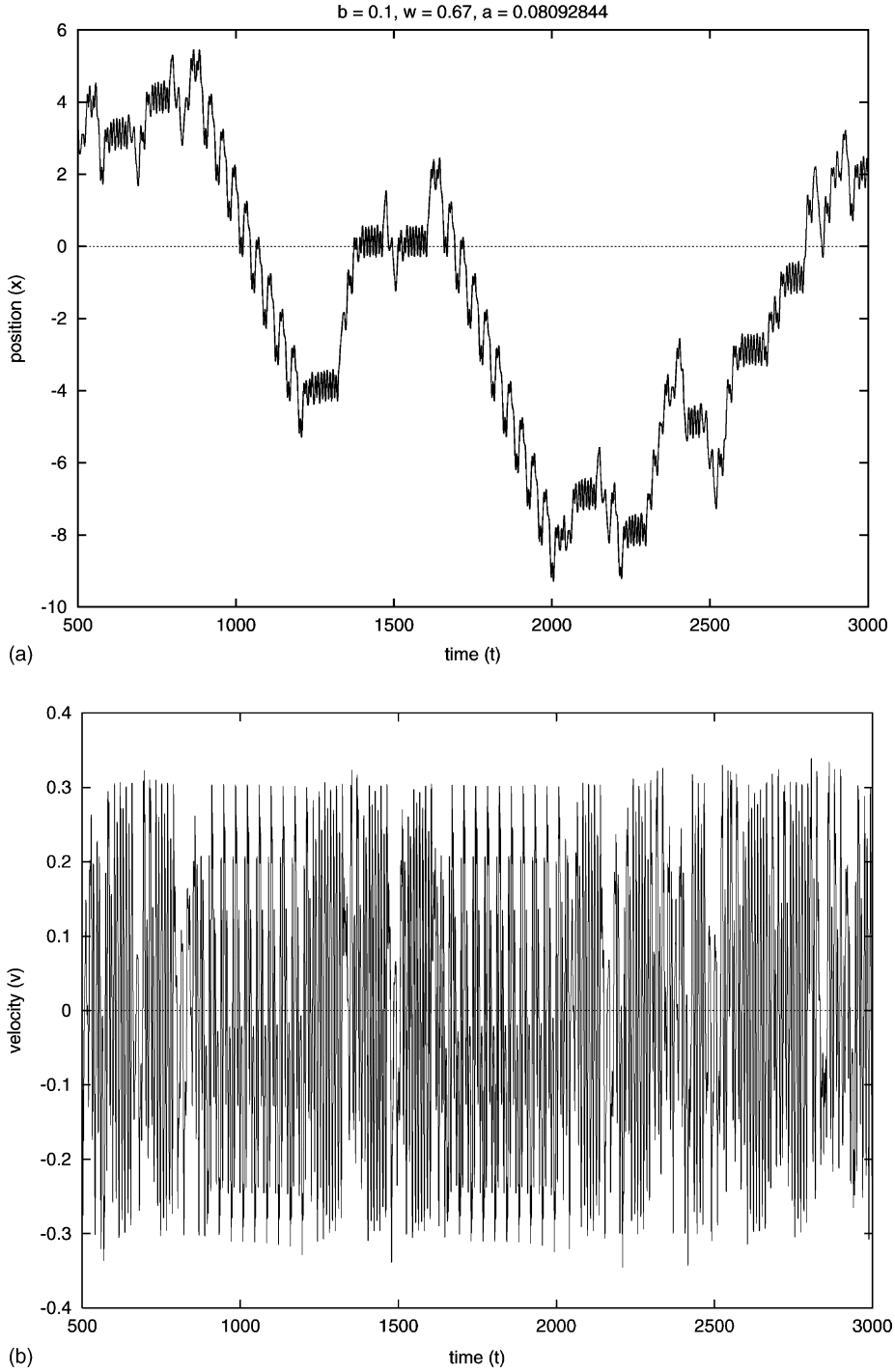

Fig. 6. For $b = 0.1$, $w = 0.67$ and $a = 0.08092844$ we show: (a) the trajectory of the particle as a function of time, (b) the velocity as a function of time and (c) the phase space. This case corresponds to a near the bifurcation, where the dynamics becomes intermittent and there is anomalous diffusion.

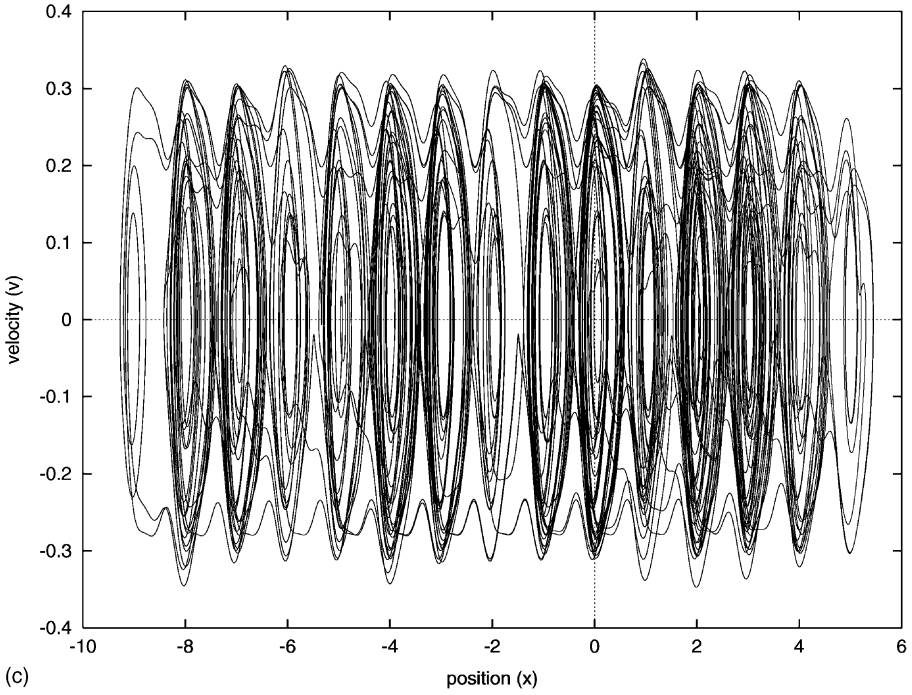

Fig. 6. (*Continued*).

exponent $\alpha \simeq 3/2$. This is a signature of anomalous deterministic diffusion, in which $\langle (x - \langle x \rangle)^2 \rangle$ grows faster than linear, i.e., $\alpha > 1$ (superdiffusion). Normal deterministic diffusion corresponds to $\alpha = 1$. In contrast, the trajectories in Figs. 4a and 5a transport particles in a ballistic way, with $\alpha = 2$. The relationship between anomalous deterministic diffusion and intermittent chaos has been explored recently, together with the connection with Lévy flights (see the reviews [26–28]). The signature of this anomalous diffusion can be seen more clearly in Fig. 6a, where we plot a trajectory showing running modes of different sizes, typical from Lévy flights.

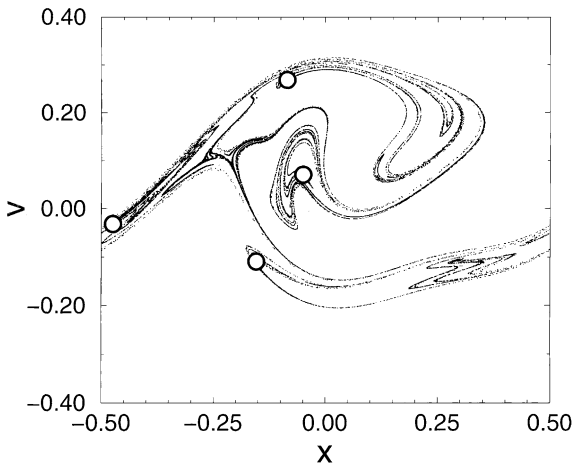

Fig. 7. For $b = 0.1$ and $w = 0.67$ we show two attractors: a chaotic attractor for $a = 0.08092$, just below a_c, and a period-4 attractor, for $a = 0.08093$, consisting of four points located at the center of the open circles (see Ref. [6]).

4. Extended objects: rigid dimers

Let us consider now the case where we have, instead of a point particle, an extended rigid dimer of length d, i.e., two point particles kept rigidly at a fixed distance d. If we define a dimensionless length $l = d/L$, where L is the periodicity of the ratchet potential in Eq. (2), the dynamics of this dimer in the ratchet potential is equivalent to the dynamics of a point particle in an effective potential given by

$$U_l(x) = \tfrac{1}{2}[V(x) + V(x + l)], \tag{8}$$

where $V(x)$ is the dimensionless potential in Eq. (4). Due to the periodicity of the dimensionless ratchet potential $V(x+1) = V(x)$, we have that the effective dimensionless potential is periodic: $U_l(x+1) = U_l(x)$. Since the period is 1, it is enough to take the dimensionless length of the rigid dimer in the unit interval: $0 \leq l \leq 1$. We can see that we recover the point particle case when $l = 0$ or 1. The equation of motion for this dimer is then given by

$$\ddot{x} + b\dot{x} + \frac{\mathrm{d}U_l(x)}{\mathrm{d}x} = a\cos(wt). \tag{9}$$

In this case, we have an additional parameter l in the dynamics. According to this equation of motion, the dynamics of the dimer is modeled using a single degree of freedom, since we are not considering any internal degree of freedom or rotational motion.

It is important to mention that several authors before had studied the case of a rigid dimer in a ratchet potential, in the overdamped limit. The case of a single rigid dimer in the overdamped limit in the presence of noise was studied in [29,30]. They obtain a current reversal as a function of the dimer length. Also, in the overdamped limit, there are studies of the collective transport of N rigid rods of finite size; these rods are interacting through hard core repulsion [31,32]. For an overview of the collective transport in ratchets, see [3,4,33].

More recently, the problem of horizontal transport of vertically vibrated granular layers on a ratchet was addressed [34,35]; it was found that increasing the layer thickness leads to a reversal of the current. Farkas et al. [36] studied the case of granular binary mixtures where, unlike other segregation phenomena, in which the segregation is due to the collective behavior of the grains, the interaction between the ratchet and the individual particles is dominant. If the density of particles is low, the interaction between the objects can be neglected, recovering a single rod description. Finally, Wambaugh et al. [37] perform simulations of elongated grains on a vibrating ratchet-shaped base; they consider grains composed of one (monomers), two (dimers) or three (trimers) collinear spheres. For some parameters, they found that monomers and dimers move in opposite directions.

In this section, we are considering the underdamped determinist dynamics of a rigid dimer. We solve the problem of the rigid dimer in the same fashion as the point particle, but instead of calculating the current J defined in Section 2, we calculate the time average of the velocity $v = \dot{x}$. This average is calculated over q periods T of the external force, where q is an integer number and $T = 2\pi/w$. That is,

$$\bar{v} = \frac{1}{qT}\int_t^{t+qT} v(t')\,\mathrm{d}t'. \tag{10}$$

Since $v = \dot{x}$, we obtain $\bar{v} = [x(t+qT) - x(t)]/qT$. If the particle moves a distance p in a time qT, where p is another integer number, then we have the condition $x(t+qT) - x(t) = p$. Thus, we obtain that the current is $T\bar{v} = p/q$. This means that we have *frequency locking* in which the current times the period T is a rational number p/q. We will see that this frequency locking takes place in a whole range of values of the parameter l.

In Fig. 8a, we show the bifurcation diagram as a function of l in the unit interval, and in Fig. 8b the corresponding average velocity in the same range. We use the following values for the parameters: $a = 0.074$, $b = 0.1$ and $w = 0.67$. We obtain a rich structure of bifurcations when we vary the size of the rigid dimer. We notice the presence of periodic and chaotic orbits. As a consequence of the complexity of the bifurcation diagram, we obtain an average velocity with fine structure. Again, there is a clear connection between the two graphs.

Let us briefly describe this connection in some detail. For very small values of l we have a positive velocity fluctuating around $T\bar{v} = 1/2$, associated with the period-2 orbit in the bifurcation diagram. After another bifurcation, the dynamics becomes chaotic for $l \simeq 0.05$ and the average velocity decreases abruptly. For the chaotic region $0.05 < l < 0.2$, the current decrease even more in an erratic way, except for a "jump" in the current around $l = 0.18$, clearly associated with a periodic window in the bifurcation diagram. Then, for $l \simeq 0.2$, a crisis bifurcation occurs in which the chaotic attractor collapses to a period-1 attractor. The periodic orbit is such that the average velocity is zero. However, we reach another crisis

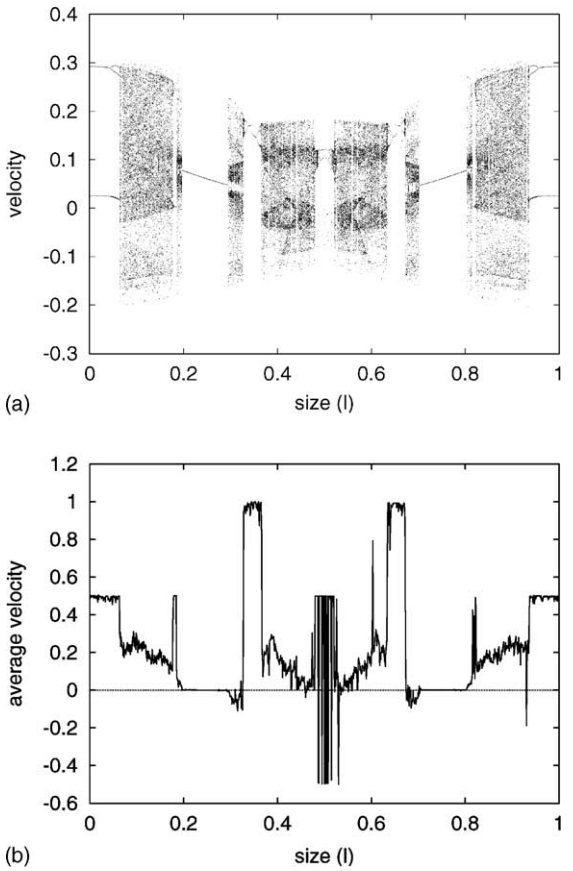

Fig. 8. For $a = 0.074$, $b = 0.1$ and $w = 0.67$ we show: (a) the bifurcation diagram of the rigid dimer as a function of l and (b) the average velocity $T\bar{v}$ of the rigid dimer as a function of l, in the same range.

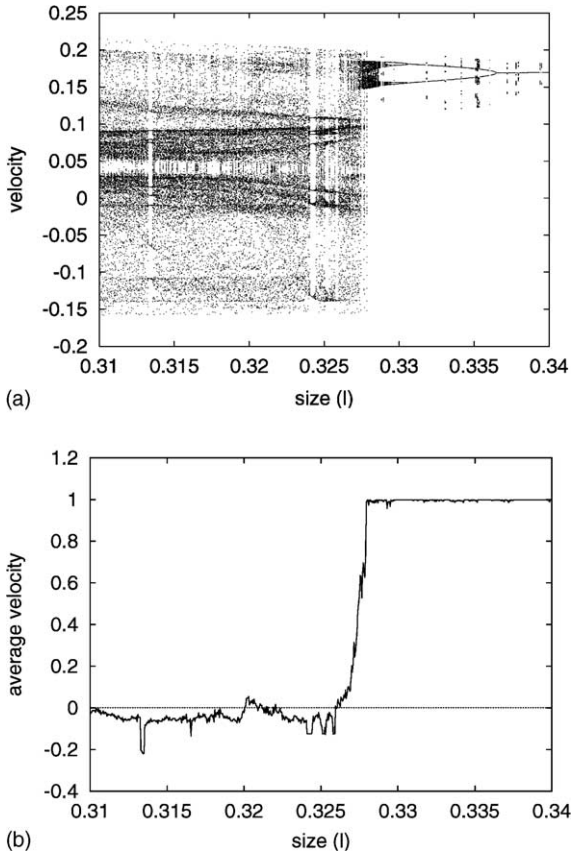

Fig. 9. For $a = 0.074$, $b = 0.1$ and $w = 0.67$ we show a detailed amplification of Fig. 8 in the size interval $[0.31, 0.34]$: (a) the bifurcation diagram of the rigid dimer as a function of l and (b) the average velocity $T\bar{v}$ of the rigid dimer as a function of l, in the same range.

to a chaotic region, around $l \simeq 0.3$, that generates a *negative current*. This negative current is maintained during the chaotic region between $l \simeq 0.30$ and $l \simeq 0.33$. However, around this value, there is again another crisis bifurcation, in which the chaotic attractor reduces in size and this bifurcation produces a *current reversal*: the current "jumps" in an abrupt way to reach values fluctuating around $T\bar{v} = 1$. The connection follows in the same fashion for larger values of l.

In Fig. 9, we show in more detail the bifurcation diagram and the average velocity, as a function of l, in the range $[0.31, 0.34]$, where a current reversal occurs. We notice more clearly the connection between the current reversal and a crisis bifurcation, around $l \simeq 0.327$, where the chaotic attractor suddenly reduces in size. Finally, in Fig. 10, we show two trajectories for two dimers of different size. Even though the size is almost the same, the dimers move apart. The dimer with $l = 0.3275$ has a positive average velocity, according to Fig. 9b, while the dimer with $l = 0.3250$ has a negative average velocity. Both trajectories are chaotic, as can be seen in the bifurcation diagram in Fig. 9a. This implies that two dimers, starting at the same point with zero velocity, separate from each other, even when the size difference is very small. In this way we can think of a possible mechanism for segregation of particles according to its size, even for the same mass.

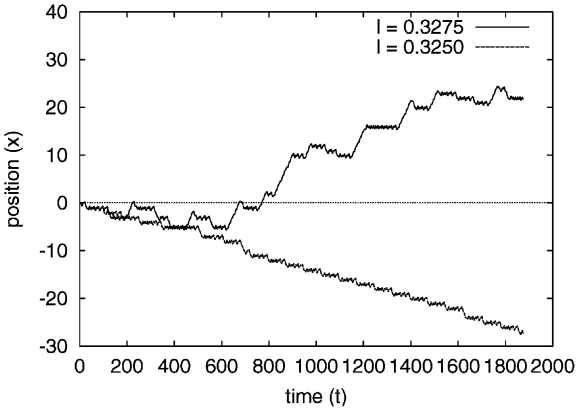

Fig. 10. For $a = 0.074$, $b = 0.1$ and $w = 0.67$ we show two trajectories for two dimers of different size. The full line corresponds to a dimer with $l = 0.3275$ (positive current) and the dashed line to a dimer with $l = 0.3250$ (negative current).

5. Concluding remarks

In summary, we have studied the chaotic dynamics of point particles and extended rigid dimers in a ratchet potential under the influence of an external periodic force. We established a connection between the bifurcation diagram and the current, and identified the mechanism by which the current reversals in deterministic ratchets arise: it corresponds to bifurcations, usually from a chaotic to a periodic regime. Near this crisis bifurcations, the chaotic trajectories exhibit intermittent chaos and the transport arises through deterministic anomalous diffusion with an exponent greater than 1. We also studied the dynamics of dimers of finite size and found that the ratchet can transport these dimers in opposite directions, even when the size difference is very small. Thus, by establishing a connection between bifurcations in the nonlinear dynamics and current reversals, this work can shed some light in the problem of segregation of granular media using the ratchet effect.

Acknowledgements

The author gratefully acknowledges financial support from UNAM through project DGAPA-IN-111000.

References

[1] P. Hänggi, R. Bartussek, in: J. Parisi, S.C. Müller, W. Zimmermann (Eds.), Nonlinear Physics of Complex Systems, Lecture Notes in Physics, Vol. 476, Springer, Berlin, 1996, pp. 294–308.
[2] R.D. Astumian, Science 276 (1997) 917.
[3] F. Jülicher, A. Ajdari, J. Prost, Rev. Mod. Phys. 69 (1997) 1269.
[4] P. Reimann, Phys. Rep. 361 (2002) 57.
[5] P. Jung, J.G. Kissner, P. Hänggi, Phys. Rev. Lett. 76 (1996) 3436.
[6] J.L. Mateos, Phys. Rev. Lett. 84 (2000) 258.
[7] J.L. Mateos, Acta Phys. Polonica B 32 (2001) 307.
[8] M. Porto, M. Urbakh, J. Klafter, Phys. Rev. Lett. 84 (2000) 6058.
[9] M. Porto, M. Urbakh, J. Klafter, Phys. Rev. Lett. 85 (2000) 491.
[10] S. Flach, O. Yevtushenko, Y. Zolotaryuk, Phys. Rev. Lett. 84 (2000) 2358.
[11] O. Yevtushenko, S. Flach, Y. Zolotaryuk, A.A. Ovchinnikov, Europhys. Lett. 54 (2001) 141.
[12] M. Barbi, M. Salerno, Phys. Rev. E 62 (2000) 1988.
[13] M. Barbi, M. Salerno, Phys. Rev. E 63 (2001) 066212.
[14] C.M. Arizmendi, F. Family, A.L. Salas-Brito, Phys. Rev. E 63 (2000) 061104.
[15] H.A. Larrondo, F. Family, C.M. Arizmendi, Physica A 303 (2002) 67.
[16] S. Cilla, F. Falo, L.M. Floría, Phys. Rev. E 63 (2001) 031110.
[17] G. Carapella, Phys. Rev. B 63 (2001) 054515.
[18] G. Carapella, G. Costabile, Phys. Rev. Lett. 87 (2001) 077002.
[19] E. Goldobin, A. Sterck, D. Koelle, Phys. Rev. E 63 (2001) 031111.
[20] G. Carapella, G. Costabile, R. Latempa, N. Martucciello, M. Cirillo, A. Polcari, G. Filatrella, cond-mat/0112467 (27 Dic 2001), Physica C, in press.
[21] B. Nordén, Y. Zolotaryuk, P.L. Christiansen, A.V. Zolotaryuk, Phys. Rev. E 65 (2001) 011110.
[22] T. Dittrich, R. Ketzmerick, M.-F. Otto, H. Schanz, Ann. Phys. (Leipzig) 9 (2000) 755.
[23] H. Schanz, M.-F. Otto, R. Ketzmerick, T. Dittrich, Phys. Rev. Lett. 87 (2001) 070601.
[24] H. Linke, T.E. Humphrey, R.P. Taylor, A.P. Micolich, R. Newbury, Phys. Scripta T90 (2001) 54.
[25] E. Ott, Chaos in Dynamical Systems, Cambridge University Press, Cambridge, 1993.
[26] M.F. Shlesinger, G.M. Zaslavsky, J. Klafter, Nature (London) 363 (1993) 31.
[27] M.F. Shlesinger, G.M. Zaslavsky, J. Klafter, Phys. Today 49 (2) (1996) 33.
[28] T. Geisel, in: M.F. Shlesinger, G.M. Zaslavsky, U. Frisch (Eds.), Lévy Flights and Related Topics in Physics, Lecture Notes in Physics, Vol. 450, Springer, Berlin, 1995, 153 pp.
[29] T.E. Dialynas, G.P. Tsironis, Phys. Lett. A 218 (1996) 292.
[30] T.E. Dialynas, K. Lindenberg, G.P. Tsironis, Phys. Rev. E 56 (1997) 3976.

[31] I. Derényi, T. Vicsek, Phys. Rev. Lett. 75 (1995) 374.
[32] I. Derényi, A. Ajdari, Phys. Rev. E 54 (1996) R5.
[33] I. Derényi, P. Tegzes, T. Vicsek, Chaos 8 (1998) 657.
[34] Z. Farkas, P. Tegzes, A. Vukics, T. Vicsek, Phys. Rev. E 60 (1999) 7022.
[35] M. Levanon, D.C. Rapaport, Phys. Rev. E 64 (2001) 011304.
[36] Z. Farkas, F. Szalai, D.E. Wolf, T. Vicsek, Phys. Rev. E 65 (2002) 022301.
[37] J.F. Wambaugh, C. Reichhardt, C.J. Olson, Phys. Rev. E 65 (2002) 031308.